SECOND EUROPEAN CONFERENCE ON EARTHQUAKE ENGINEERING AND SEISMOLOGY, ISTANBUL AUG. 25-29, 2014

NUMERICAL STUDY OF URM INFILLED REINFORCED CONCRETE FRAME RETROFITTED WITH EMBEDDED REINFORCING STEEL

Rajendra SOTI[1], Andre R. BARBOSA [2] and Andreas STAVRIDIS [3]

ABSTRACT

Unreinforced masonry (URM) infill walls are widely used in regions with high seismicity around the world. When subjected to seismic loading, the failure of these walls is often catastrophic as these walls typically exhibit brittle failures. These catastrophic failures have been observed since earthquakes in the 1930s and also in the aftermath of recent earthquakes such as the 2010 Haiti (Mw 7.0), the 2010 Maule Chile (Mw 8.8), and the 2010 and 2011 Darfield and Christchurch New Zealand earthquakes (Mw 7.1 and Mw 6.3, respectively). All the failures observed should be reason enough for retrofitting of URM and URM infill RC frames, but the cost is typically the main hindrance to seismically upgrading these URM walls. Thus, there still is a pressing need for developing cost-effective retrofit strategies.

A simple and cost-effective retrofit solution for URM infill walls is proposed herein, in which embedded reinforcing steel bars are placed in pre-cut grooves made on the surface of the infill walls. The proposed retrofitting technique is assessed through the use of nonlinear finite element analyses. In these analyses, a modelling scheme consisting of smeared and discrete crack approaches are combined to capture the different failure modes of infilled frame, including mixed-mode fracture of mortar joints and column shear failure of reinforced concrete (RC) members. The modelling approach is validated through correlation of experimental results with numerical results obtained herein for a one-bay, one-story specimen. Numerical results of retrofitted one and two-bay retrofitted masonry infills illustrate that horizontal reinforcements are more effective than vertical reinforcements when retrofitting URM walls. Results are promising, but uncertainties suggest that experimental testing needs to be done before conclusions on the efficiency of the retrofitting method can be drawn.

INTRODUCTION

All over the world, unreinforced masonry walls are used extensively as infill wall panels in reinforced concrete frame structures. In the design process, the capacity of the walls are not considered in the design of the lateral resisting system since these infill walls are considered as non-structural elements and are usually overlooked. However, past earthquakes have repeatedly indicated the catastrophic

[1] Graduate Student Researcher, School of Civil & Construction Engineering, Oregon State University, Corvallis, sotir@onid.orst.edu
[2] Assistant Professor, School of Civil & Construction Engineering, Oregon State University, Corvallis, Andre.Barbosa@onid.orst.edu
[3] Assistant Professor, Dept. of Civil, Structural & Environmental Engineering, University of Buffalo, Buffalo astavrid@buffalo.edu

brittle failure of infill masonry panels and that they affect the mechanisms of failure of the reinforced concrete frame structure. Improving the seismic performance of these infill walls, by increasing the ductility using the cost-effective retrofitting technique is a promising way to address this problem. This paper proposes a new cost-effective solution for seismic retrofit of URM infill walls by providing embedded horizontal and/or vertical reinforcing steel bars into pre-cut grooves. The proposed retrofitting method can be applied efficiently and causes minimum disruption to occupants as well as little architectural impact. The techniques discussed here have minimum impact on the aesthetics of the retrofitted URM walls since the strengthening system is hidden inside the wall. In this preliminary assessment, advanced nonlinear finite element analyses are used to assess the proposed solution.

Significant advancement has been made on nonlinear finite-element modelling of concrete and masonry structures. Modelling techniques can be classified into phenomenological models (Burton and Deierlein, 2013) or advanced continuum models such as the ones developed in Stavridis and Shing (2010). Burton and Deierlein (2013) have proposed an inelastic dual-strut model that captures the post-peak behaviour of the masonry infill and its interaction with the surrounding frame. This follows many works that include strut-and-ties to capture the brittle behaviour of the infill. Phenomenological models are effective, but only for capturing global behaviour. Furthermore, these have to be calibrated to experimental results. In the absence of these experimental results, advanced continuum models should be used since these are more reliable, yet computationally expensive. An example of such continuum models is the one by Stavridis and Shing (2010). In this model the authors use a nonlinear modelling scheme that combines smeared-crack continuum elements with interface elements to simulate the fracture behaviour of unreinforced masonry-infilled RC frames. The smeared crack and interface models have been implemented in the Finite Element Analysis Program (FEAP, Taylor 2007). Smeared crack elements (Lotfi and Shing 1991) were used to model the concrete in the RC frame and masonry units in the infill panel. Interface models (Lotfi and Shing 1994) were used to capture the mixed-mode fracture of mortar joint and shear failure of RC members.

The modelling technique by Stavridis and Shing (2010) were validated with experimental data for non-retrofitted, one-bay, one-story, reinforced concrete frames with masonry infills. Herein, the same modelling approach is applied to the assessment of a retrofitting strategy, with one minor extension. The reinforcing steel bars used in the retrofit are embedded in URM infill walls to upgrade its structural performance. Retrofitting cases considered include use of horizontal and/or vertical reinforcement in one-bay frame and use of horizontal bars in two-bay infill frame. The embedded reinforcements are modelled with elasto-plastic truss elements and are placed parallel to the mortar joints. Effects of dowel action are neglected. Performance of non-retrofitted URM infill RC frame and the retrofitted URM infill RC frame are compared based on static pushover analysis results. Results suggest this solution can be efficient.

PROPOSED RETROFIT SCHEME

The retrofit approach proposed herein involves the installation of reinforcing steel bars into the pre-cut groves in the surface of the masonry wall. Fig. 1 a, b, and c show possible retrofit strategies. Horizontal bars are placed into pre-cut grooves, as shown in Fig. 2a. In this preliminary evaluation of the retrofitting approach, and to bound the design values, the depth of the groove has been limited to 1.0 inch and width of the groove has been made equal to the width of the mortar joints. Typically a #3 (10 mm) reinforcing steel bar fits into this groove and the bar can be bonded to the bricks and protected by filling the groove with an epoxy.

Two case studies are analysed. The first is one-bay frames shown in Fig. 1. In this first case, three retrofit strategies are analysed. The second case study consists of a two-bay RC frame with URM infill walls, as shown in Fig. 2b. In this case study, only horizontal reinforcements are provided to the masonry-infill wall. For construction ease, the horizontal bars terminate at column faces.

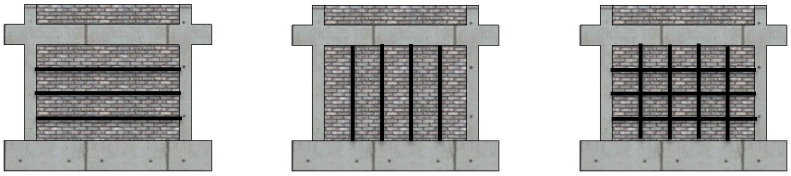

(a) (b) (c)

Figure 1. Retrofitting strategies for one bay frame: (a) retrofitted specimen with horizontal bars; (b) retrofitted specimen with vertical bars, (c) retrofitted specimen with horizontal and vertical bars

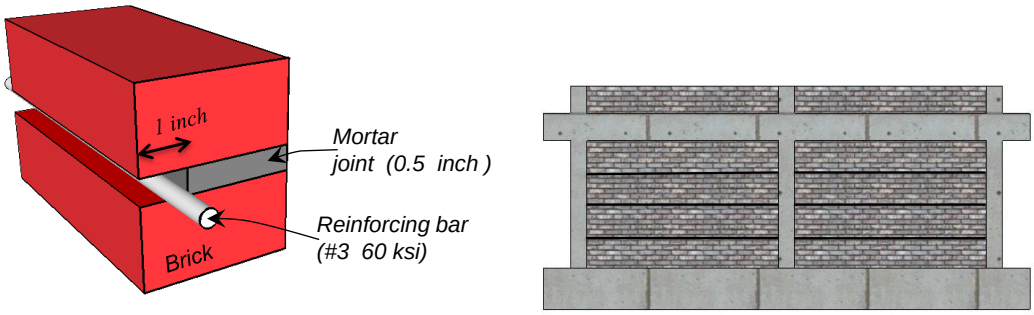

(a) (b)

Figure 2. Retrofitting strategy for two-bay frame: (a) embedded horizontal reinforcement into groove, (b) retrofitted specimen (two-bay) with horizontal bars

NUMERICAL MODELLING AND FINITE ELEMENT FORMULATION

In this section, the finite element modelling approach for URM infill RC frames used herein is summarized. The approach is based on the discretization scheme and constitutive modelling implemented in FEAP (Taylor 2007). Particular attention is given to the modelling of RC members and URM infill including the mortar and brick interfaces as well as the steel reinforcement used for retrofitting the masonry walls.

A smeared-crack finite element formulation (Lotfi and Shing 1991) is used to model concrete in RC frames as well as the masonry units in the infill panel. The concrete or brick elements are modelled with an elastic-plastic relationship governed by a von Mises two-dimensional failure surface, as shown in Fig. 3a. When the von Mises failure criterion is reached, an associated flow rule is used to compute the plastic strains. At larger plastic strains, i.e. when cracks occur, the material model adopts an orthotropic material law to simulate the nonlinear behaviour in tension and compression as shown in Fig. 3b and Fig. 3c. It is worth noting that the crack forms orthogonal to the directions of principal stresses, and once these form, the crack orientation is fixed through the analysis.

Interface elements are provided between the concrete smeared-crack elements and between the masonry brick elements. These elements correspond to four-nodded, zero-thickness, cohesive crack interface elements. The constitutive relationship used to model the interface elements is shown in Fig. 3d. This figure shows the hyperbolic yield function and its evolution, which are based on the cohesive crack formulation. As described in Lofti and Shing (1994), the cohesive crack formulation is used to simulate Mode-I, Mode-II, and mixed-mode fractures. In this model, shear dilation is also observable as this effect can dilate and contract the yield surface. At each point along the interface, the model follows an elastic-plastic formulation, given by the following flow rule:

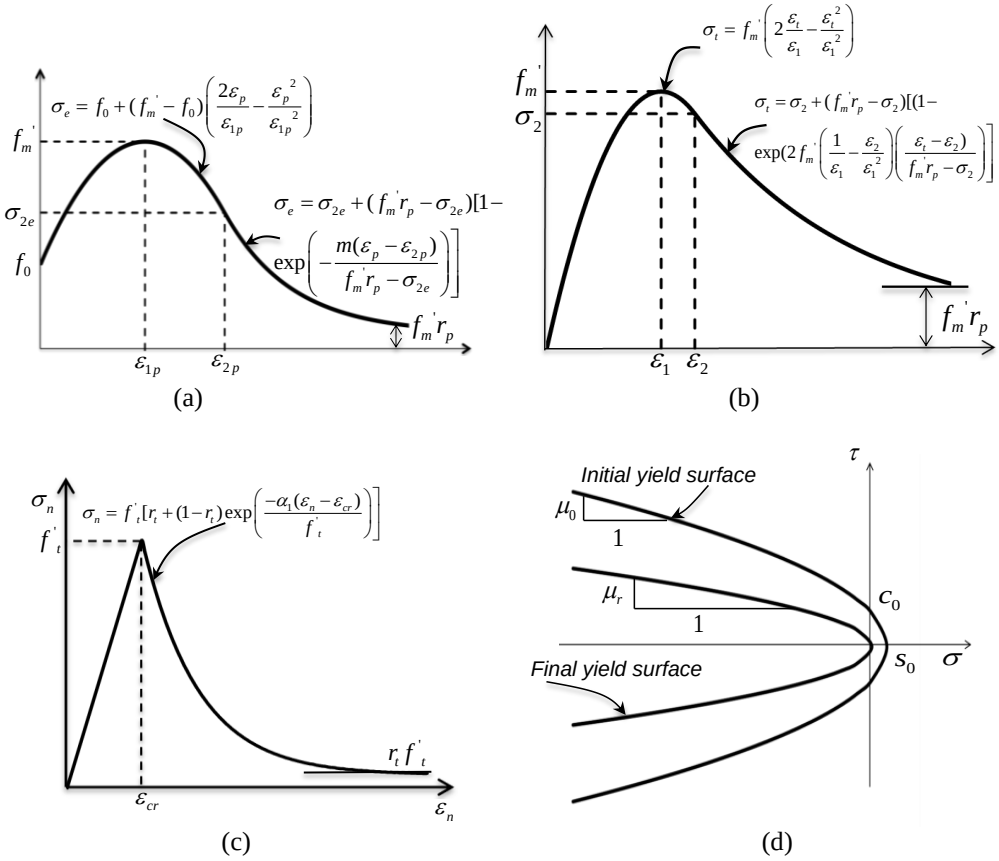

Figure 3. (a) Plasticity model, (b) compressive behavior of orthotropic model, (c) tensile behavior of orthotropic model, and (d) interface yield surface

$$\dot{\boldsymbol{\sigma}} = \boldsymbol{D}\left(\dot{\boldsymbol{d}} - \dot{\boldsymbol{d}}^{p}\right) \tag{1}$$

where $\boldsymbol{\sigma} = \{\sigma \;\; \tau\}^{T}$, σ and τ are the normal and shear stresses; $\boldsymbol{d} = \{d_n \;\; d_t\}^{T}$, and d_n and d_t are the normal and shear displacement, respectively; $\boldsymbol{D}$ is a diagonal matrix with elastic constants D_n and D_t associated with normal and tangential direction. The hyperbolic yield surface is given by:

$$F(\boldsymbol{\sigma},\boldsymbol{q}) = \tau^2 - \mu^2(\sigma - s)^2 + 2r(\sigma - s) = 0 \tag{2}$$

where μ is the slope of the asymptotes of the hyperbola, *s* is the interface tensile strength, and *r* is a radius of the yield surface at the vertex of the hyperbola, and where $\boldsymbol{q} = \{\mu, s, r\}$ groups the parameters that characterize the yield surface. The evolution of yield surface is based on the following softening rules:

$$s = s_0\left(1 - \frac{k_1}{G_f^{I}} - \frac{k_2}{G_f^{II}}\right) \geq 0,\;\; r = r_r + (r_0 - r_r)e^{-\beta k_3},\; \mu = \mu_r + (\mu_0 - \mu_r)e^{-\alpha k_3} \tag{3}$$

In Eq. 3, the subscript 0 and *r* represent the initial and residual value of the respective variables, respectively; G_f^{I} and G_f^{II} represent the Mode-I and Mode-II fracture energies; α and β control the rate of reduction of μ and r respectively; k_1, k_2, and k_3 correspond to the plastic work quantities

that govern the strength degradation from the initial to the residual parameters. The plastic potential, with a non-associated rule, is given by:

$$Q(\boldsymbol{\sigma},\boldsymbol{q}) = \eta\tau^2 + (r - r_r)(\sigma - s) \tag{4}$$

where η is a scaling parameter controlling shear dilatation. The direction of plastic displacements is governed by the flow rule, $\dot{\boldsymbol{d}}^p = \dot{\lambda}\dfrac{\partial Q}{\partial \sigma}$, where λ is the plastic multiplier.

DISCRETIZATION OF REINFORCED CONCRETE MEMBERS

The RC members of the frame are discretized in modules of four triangular smeared-crack elements connected with four, diagonally placed, interface elements as shown in Fig. 4a. The interface elements model horizontal, vertical, and diagonal shear cracks, in a discrete manner, thus allowing for discrete modelling of the cracks. The reinforcing steel bars in the concrete members are modelled with elastic-plastic truss elements. Vertical reinforcing steel have been divided into eight truss elements at each interior location and four truss elements along the external edges. Shear reinforcement bars have been divided into two bars placed in a zigzag pattern, as shown in Fig. 4a.

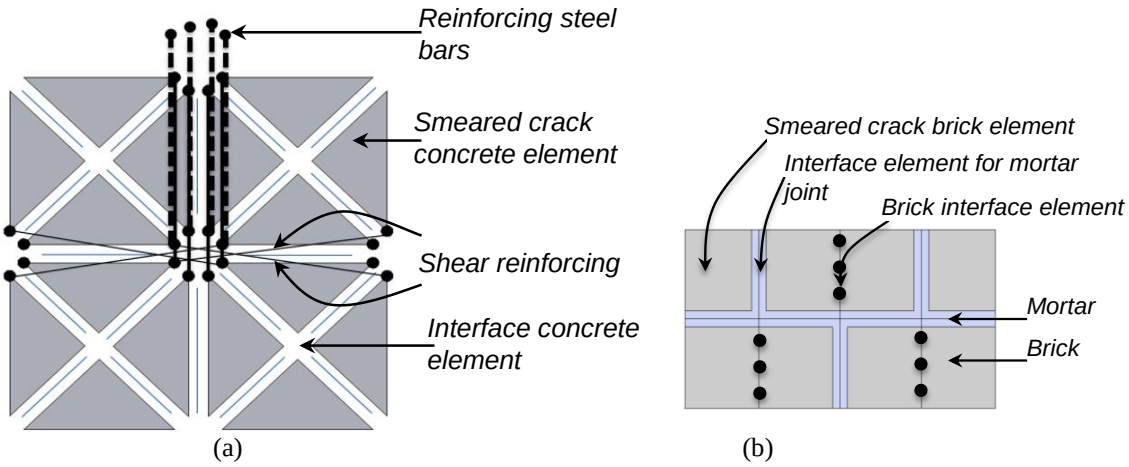

Figure 4. Finite element discretization of (a) RC members, and (b) masonry infill

DISCRETIZATION OF URM INFILL

The discretization scheme for the unreinforced masonry panel is shown in Fig. 4b. Here, each masonry unit (i.e. a single brick) is modelled with two rectangular continuum elements interconnected with a vertical interface element. The vertical interface element can capture the tensile splitting of the masonry unit and the relative sliding of a fractured unit. Mortar joints are modelled with a zero-thickness cohesive interface elements also shown in Fig. 4b.

DISCRETIZATION OF EMBEDDED REINFORCING STEEL BARS

The reinforcing bars used in the retrofitting are modelled with elasto-plastic truss elements. Each reinforcing bar is split into four truss elements connecting the nodes of continuum brick elements shown in Fig. 5. For the embedded bar, the contribution of dowel action may be important, but it has not been taken into account in this study.

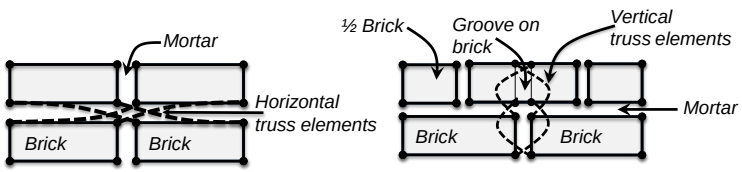

Figure 5. FEM discretization of retrofitted model

CALIBRATION OF MATERIAL MODELS

Stavridis and Shing (2010) performed a systematic calibration of the material model and a sensitivity analysis of different material parameters. Some parameters were calibrated with available material test data, other parameters are chosen carefully to capture the overall behaviour of a masonry assembly. Herein, the same calibration approach is adopted. The results of calibration of the smeared crack and interface elements for the concrete and brick are shown in Fig. 6a, b. the calibrated interface model for mortar joints is shown in Fig. 7a and b. The latter two figures illustrate that the model represents well the experimental testing in Mehrabi at el. (1994) at the level of the masonry unit.

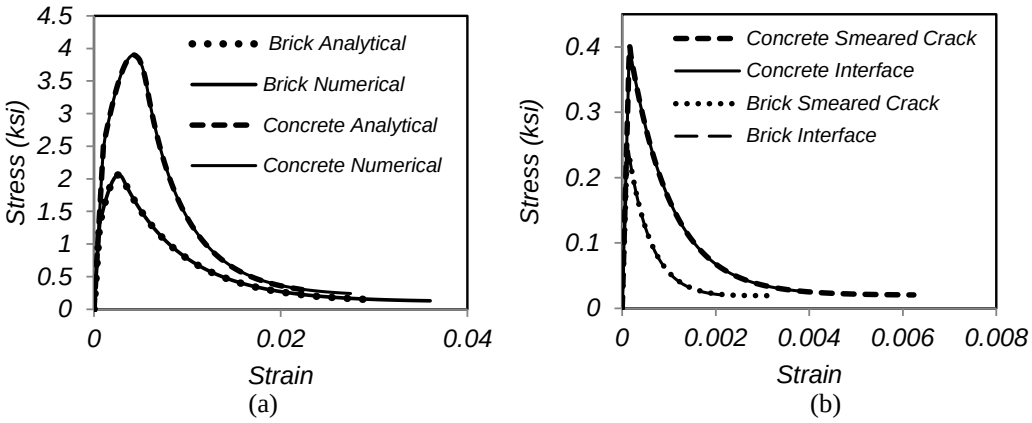

Figure 6. Calibration of smeared crack and interface for concrete and brick: (a) compressive behavior and (b) tensile behavior

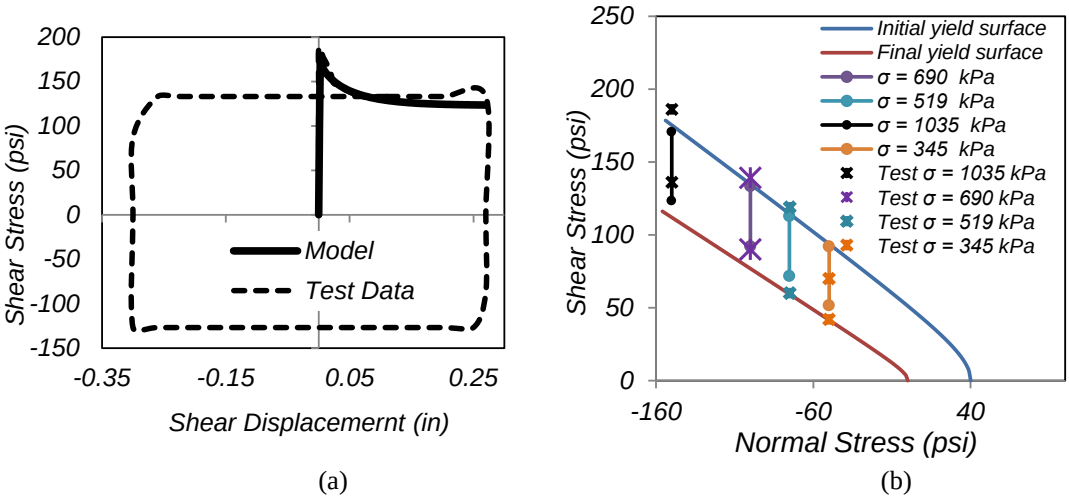

Figure 7. Shear test Mehrabi at el. (1994) calibration of interface model for mortar joints: (a) test and numerical results for σ = 159 ksi, and (b) test data and numerical initial and final yield surface

CASE STUDIES

Herein, two cases studies shown in Fig. 1 and Fig. 2 are analysed. The first case study is a one-bay masonry infill RC frame. This corresponds to Specimen 9, experimentally tested by Mehrabi (1996) and numerically analysed by Stavridis and Shing (2010). The original model did not include any retrofits and associated reinforcement. It was designed for wind loads as per ACI 318-89. The frame was loaded laterally by an actuator moving in displacement control. The size of the brick unit was 92mm x 92mm x 194mm. The second case study corresponds to a two-bay masonry infill frame model. The design and detailing of the two-bay frame model is shown in Fig. 8. This case study is an extension of the Mehrabi (1996) design. P_1 through P_3 are locations where loads are applied. The test and analysis is done by controlling the displacement at and in the direction of P_1. The values of the vertical loads are identical to the ones in Mehrabi (1996).

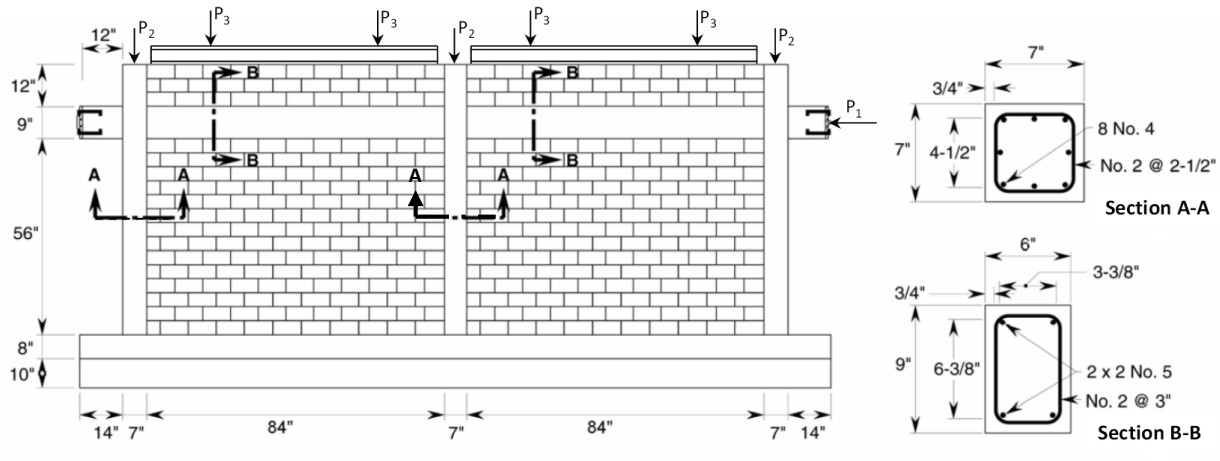

Figure 8. Design and detailing of two-bay infill frame

VALIDATION OF THE MODELING APPROACH

Fig. 9a shows the test result for non-retrofitted one-bay infill frame and the numerical results (in dotted line). It can be seen that the numerical model captures very well the capacity of the test specimen, and reasonably well the initial stiffness. However, the numerical model is stiffer than the experiment and therefore the peak strength is reached for a smaller drift than the corresponding peak strength-drift value observed in the test. Currently, in the absence of experimental results for the two-bay frame as well for the retrofitted cases, no validation of the numerical results is possible, beyond checks that the results seem realistic. Nonetheless, it is suggested that further experimental works are needed.

NUMERICAL RESULTS

One-bay frame

Fig. 9 shows the individual contribution of three different retrofitting strategies shown in Fig. 1. As indicated in that figure, all retrofitted models showed a significant increase in post–peak system ductility. All retrofitted models, except the model retrofitted with four vertical bars, showed an increase in shear capacity when compared to the non-retrofitted model. The reduction of peak strength of retrofitted specimens with four vertical reinforcements indicates the change in failure pattern due to the presence of grooves cut into the surface of the wall to encapsulate the reinforcing bars (see Fig. 10 and more detailed discussion below). The force-deflection behaviour of different models is summarized in Table 1.

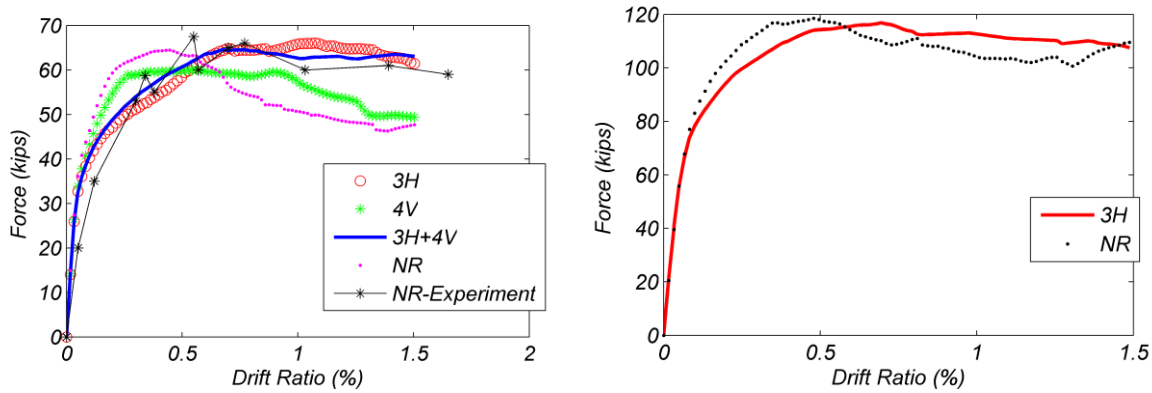

Figure 9. Load displacement curves one bay frame: (a) one-bay frame and (b) two-bay frame

Table 1: Numerical results of non-retrofitted and retrofitted specimens (one-bay frame)

Specimen	Yield point		Peak load		Residual strength (90 % of peak load)	
	$V_{y=}2/3\ V_{max}$ (kips)	δ_y (in)	V_{max} (kips)	δ_{Vmax} (in)	V_{res} (kips)	δ_{vres} (in)
Non-retrofitted (NR)	43.2	0.06	64.8	0.27	58.32	0.40
Retrofitted with 3 horizontal bars (3H)	45.43	0.09	68.15	0.72	61.3	0.9
Retrofitted with 4 vertical bars (4V)	42	0.08	63	0.47	56.7	0.66
Retrofitted with 3 horizontal + 4 vertical bars (3H+4V)	40.0	0.05	59.91	0.45	53.91	2

The failure patterns of retrofitted and non-retrofitted models are shown along with the deformed shapes in Fig. 10. In the non-retrofitted one-bay frame, a sudden diagonal crack occurred at peak load predominantly through mortar joints in a diagonal step pattern model, followed by a rapid reduction of load carrying capacity. Rapid decrease in load carrying capacity after the peak load indicates the brittle nature of unreinforced masonry infill. This can be confirmed by Fig. 9a, Fig. 10a and 10b. The left most column of Fig. 10 shows the deformed shape and crack pattern at 0.5% drift ratio, for all models. All retrofitted models improved the performance without (apparently) being damaged and with no sudden drop in load carrying capacity (see Fig. 9b and Fig. 10c, 10e, 10g).

With increasing drift ratio, non-retrofitted infill wall exhibited a gradually increasing crack width, followed by severe slip failures along a bed joints in the infill (see Fig 10b). The right most column of Fig. 10 shows the deformed shapes and crack patterns at 1.5% drift ratio. In this figure, and at this level of drift ratio, the non-retrofitted model suffered heavy damage with the formation of the wide diagonal shear cracks and severe slip failures in bed joints (Fig. 10b). Shear failure also observed at the top part of the windward column and the bottom part of the leeward column. URM infilled RC frame that is retrofitted using three horizontal reinforcing bars exhibited behaviour that is substantially more ductile in comparison to the non-retrofitted model. Cracking through this model typically initiated at approximately peak load, which was reached near 1% drift ratio. With further increase in load, a significant number of distributed diagonal cracks along with slip failure along a bed joints in the infill are observed which can be confirmed in Fig. 10d. For a retrofitted model with four vertical reinforcing bars, cracking initiated at 0.56 % drift ratio and distributed vertical cracks are observed at 1.5% drift ratio (see Fig. 10f). This model exhibited less shear resistance than the non-retrofitted model, but it exhibited better performance by increasing the post-peak system ductility. It is worth noting that the failure patterns of the retrofitted masonry wall depend on the predominant resisting failure mechanism. Due the opening of cracks, since horizontal bars are more effective resisting shear

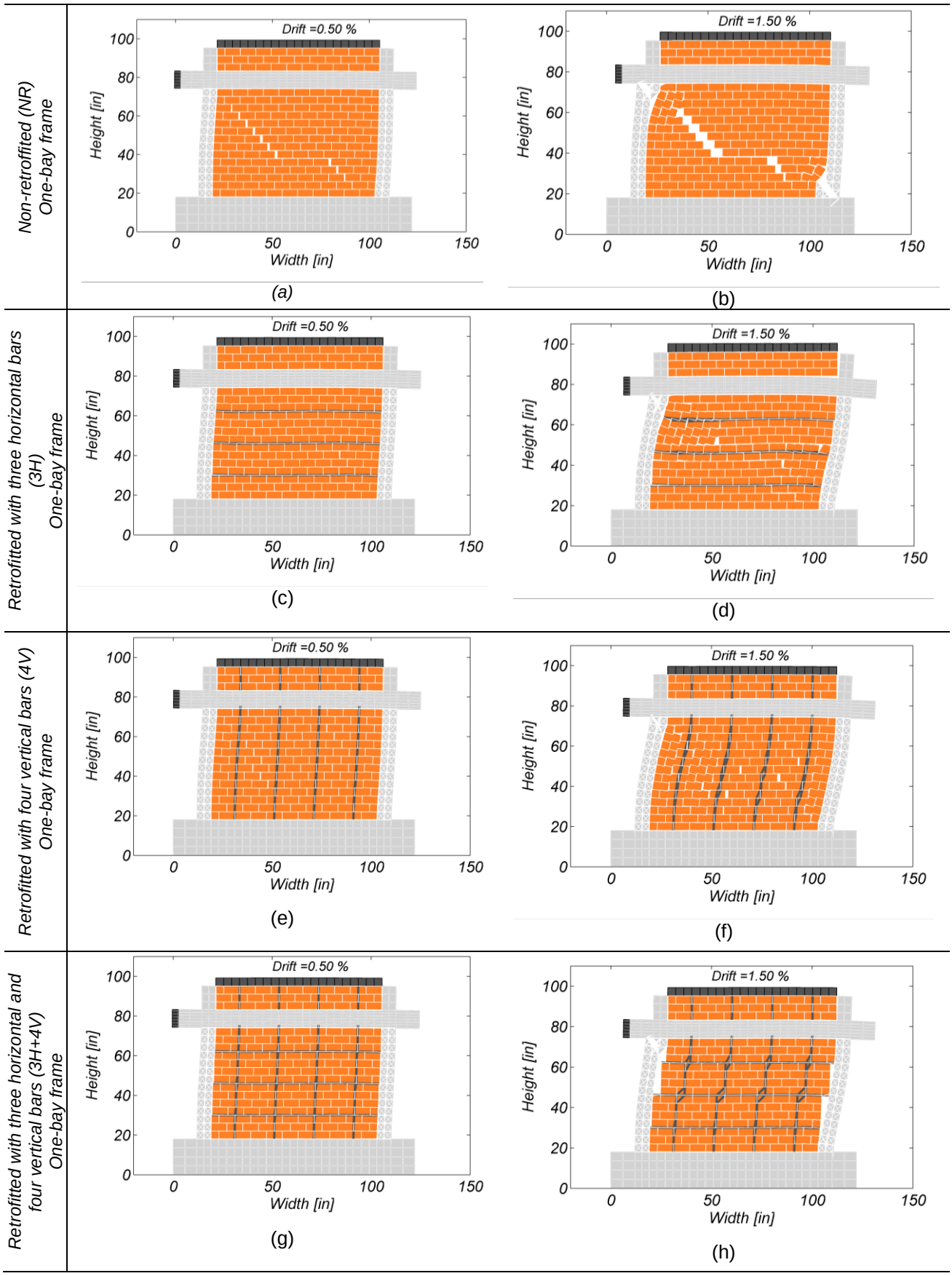

Figure 10. Deformed shape of one-bay frame

than vertical bars, bars provided better resistance against the in-plane loading. Lastly, and as expected, the retrofitted model with three horizontal and four vertical bars exhibited better performance with a substantial increase in ductility and deformation capacity. Cracking patterns of this model are shown in Fig. 10g and Fig. 10h, at 0.5% and 1.5% roof drift ratios, respectively. The combined action of horizontal and vertical reinforcing bars allowed the sliding failure along the bed joints and ultimately increased the ductility of the system.

Two-bay frame

Fig. 9b shows the influence of the horizontal bars in a two-bay URM infilled RC frame. The three horizontal bars retrofit option was selected since it corresponds to the easiest retrofit method to implement in practice. As shown in this figure, retrofitted specimen actually achieved approximately same lateral strength capacity as the non-retrofitted model. However, the post-peak system ductility is improved when reinforcing bars are added. A sudden diagonal crack along with the sliding failure along the bed joints is observed in non-retrofitted model at 0.5 % drift ratio, which can be seen in Fig. 11. With increasing drift ratio, a rapid reduction in load carrying capacity is observed (see Fig. 9b). However, the retrofitted model with three horizontal bars sustained damage at 0.5% drift ratio without losing load carrying capacity (see Fig. 9b and Fig. 11c) and the peak load occurs at approximately 0.72% drift ratio. Cracking patterns of the non-retrofitted two-bay URM infilled RC frame model at 1.5% drift ratio is shown in Fig. 11b. Non-retrofitted specimen suffered severe damaged with wide opening of cracks and shear failure of columns. Crushing of bricks can also be observed at top right and bottom left corner of the wall. At the same drift ratio, presence of horizontal bars in the retrofitted model provided a better distribution of stresses in the walls and only few distributed cracks allowed (see Fig.11d). The force-deflection behaviour of different models is summarized in Table 2.

Table 2: Numerical results of non-retrofitted and retrofitted specimens (two-bay frame)

Specimen	Yield point		Peak load		Residual strength (90 % of peak load)	
	$V_{y=}2/3\ V_{max}$ (kips)	δ_y (in)	V_{max} (kips)	δ_{Vmax} (in)	V_{res} (kips)	δ_{vres} (in)
Non-retrofitted (NR)	79.02	0.09	118.53	0.48	106.68	0.93
Retrofitted with 3 horizontal bars (3H)	77.90	0.09	116.86	0.72	105.17	1.6

CONCLUSIONS

A simple and cost effective retrofit solution consisting of reinforcing steel bars embedded into the pre-cut grooves in the surface of the masonry wall is proposed. An advanced nonlinear finite element is used to predict the efficiency of the proposed retrofitting technique. In this work, on a first phase, pushover analysis is conducted on non-retrofitted one-bay, one story URM infilled RC frame model and it is validated with test results available in from the literature. Very good agreement is found between the numerical force-displacement diagram and the monotonic experimental envelope describing the in-plane force-displacement behaviour of URM infilled RC frame. The validated non-retrofitted model is the retrofitted using different sets of reinforcing bars, which included three horizontal bars (3H), four vertical bars (4V), and three horizontal bars and four vertical bars (3H+4V). The bars consisted of a 3/8 inch diameter reinforcing steel bar (~10 mm diameter). Using these retrofit solutions the 3H and 3H+4V cases showed improvements in terms of ductility of the system, while maintaining similar lateral resistance. Based on the analysis, for the one-bay frame it is concluded that the retrofitted specimen using both horizontal and vertical embedded reinforcing bars provided the best performance in terms of ductility and deformation capacity. In a second phase, the one-bay model is extended to the two-bay model with a similar design consideration. In this work, only the case in

which the walls are retrofitted with three horizontal bars was considered. Individual contribution of each retrofitting cases is analysed and compared. Furthermore it is observed that the influence of horizontal bars is substantially higher than the influence of vertical bars in the performance of the retrofitted model. In future works, the effect of also considering the vertical bars will also be considered.

Although this study is restricted to numerical analysis, it provides a good insight for the future works, namely related to incorporation of dowel-action (Koutromanos et al., 2011), and development of simplified methods for analysis of retrofitted masonry-infill RC frames (Burton and Deierlein, 2013). Furthermore, once more data is available on different masonry and relative capacity between infills and frame is available, design and execution guides can be developed.

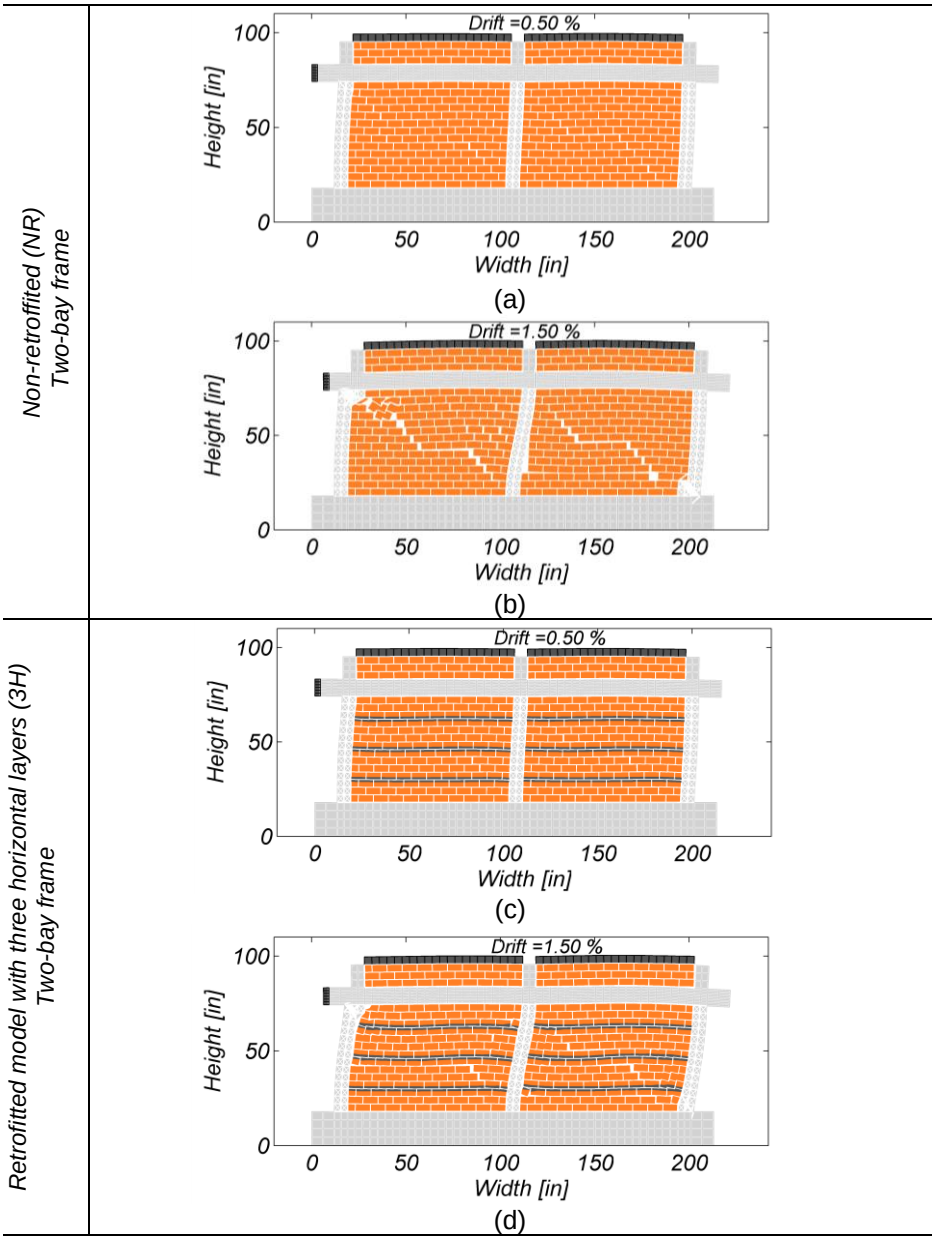

Figure 11. Deformed shape of two-bay frame

ACKNOWLEDGEMENT

The authors would like to acknowledge the support of Cascadia Lifelines Program (CLiP). The second author would also like to acknowledge the support of the School of Civil and Construction Engineering at Oregon State University. The opinions and conclusions presented in this paper are those of the authors and do not necessarily reflect the views of the sponsoring organizations.

REFERENCES

Burton H, Deierlein G (2013) "Simulation of Seismic Collapse in Non-Ductile Reinforced Concrete Frame Buildings with Masonry Infills", *Journal of Structural. Engineering*, 10.1061/ (ASCE) ST.1943-541X.0000921 3 August

Lotfi HR, Shing PB (1994) "Interface Model Applied to Fracture of Masonry Structures", *Journal of Structural Engineering*, 120(1): 63-80

Lotfi HR, Shing PB (1991) "An Appraisal of Smeared Crack Models for Masonry Shear Wall Analysis", *Computers and Structures*, 41(3): 413-425

Mehrabi AB, Shing PB Schuller M, Noland J (1996) "Experimental Evaluation of Masonry-Infilled RC Frames" *Journal of Structural Engineering*, 122(3):1761-1784

Mehrabi AB, Shing PB Schuller M, Noland I (1994) Performance of Masonry-infilled RIC Frames under In-plane Lateral Loads, Rep. CU/SR-94-6, Department of Civil ., Envir., and Arch

Koutromanos I, Stavridis A, Shing PB Willam K (2011) "Numerical Modelling of Masonry-infilled RC Frames Subjected to Seismic Loads", *Journal of Structural Engineering*, 89(11-12):1026-1037

Stavridis A, Shing PB (2010) "Finite-Element Modelling of Nonlinear Behavior of Masonry-infilled RC Frames" *Journal of Structural Engineering*, 136(3): 285-296

Stavridis A (2009) Analytical and Experimental Study of Seismic Performance of Reinforced Concrete Frames Infilled with Masonry Walls, Ph.D. Dissertation, Department of Structural Engineering, University of California, San Diego

Taylor RL (2007) FEAP-A Finite Element Analysis Program-Version 8.1, University of California at Berkeley, California